Double resonance Raman scattering of second-order Raman modes from an individual graphite whisker

P.H. Tan[a,*], C.Y. Hu[a], J. Dong[b], W.C. Shen[b]

[a]*State Key Laboratory for Superlattices and Microstructures, P.O. Box 912, Beijing 100083, China*
[b]*Laboratory of Advanced Materials, Department of Materials Science and Engineering, Tsinghua University, Beijing 100084, China*

Abstract

Resonant Raman scattering of second-order Raman modes from an individual graphite whisker synthesized by a high-temperature heat-treatment method at a special pressure was discussed here. The dependence of phonon frequencies on the incoming laser light and the frequency difference between Stokes and anti-Stokes scattering show their origin from double resonance Raman scattering. Our results show that all the experimental results of second-order Raman modes in graphite whiskers, such as the excitation-energy dependence on the mode frequency, the frequency shift between a second-order Raman mode and its fundamentals, and the frequency discrepancy between Stokes and anti-Stokes components of a second-order Raman mode can be well understood by double resonance Raman scattering.

1. Introduction

Monocrystalline graphite shows two Raman-active E_{2g} modes at 42 and 1582(G) cm^{-1} [1]. In the Raman spectra of disordered graphite, there are two additional first-order lines at ~1360 and 1620 cm^{-1}, which are often designated as the D and D′ modes [1], respectively. In the Raman spectra of graphite whiskers and multi-walled carbon nanotubes (MWNTs), two first-order (L$_1$ and L$_2$) modes are observed in the low-frequency region of 150–500 cm^{-1} [2,3]. Except two zone-center E_{2g} modes, the frequencies of other first-order Raman modes strongly depend on the excitation energy in a wide energy range [2–5]. Recently, the dispersive D mode and other first-order dispersive modes are assigned to the double resonance Raman scattering (DRRS) of the non-center phonons in several phonon branches of graphite [1,3,6–8]. The anti-Stokes double resonance Raman process of the D mode and other

first-order modes in graphite materials has also been investigated recently [3,6–9].

There exist also several dispersive second-order Raman modes in graphite materials. For example, excited with a red laser, the Raman spectra of graphite whiskers show their second-order Raman modes at about 450, 570, 1830, 1950, 2660 and 3240 cm^{-1} [2], some of which are also observed in other graphite materials [3,5,10]. According to the frequency match and the dispersive properties, these second-order Raman modes have been assigned to the overtones and combination modes of the observed first-order Raman modes. We have experimentally studied the Stokes and anti-Stokes Raman scatterings of second-order Raman modes in graphite, graphite whiskers and MWNTs [2,3,11]. The results exhibit three spectral features: (1) the frequency of a second-order mode may be unequal to the sum of the frequencies of its two fundamentals, (2) the value of the excitation-energy dependence of a second-order mode is almost equal to the sum of those of its fundamentals, (3) the frequency difference between second-order Stoke and anti-Stokes modes is determined by its peak frequency and dispersive property. The case of the

*Corresponding author. Tel.: +44 1223 748368; fax: +44 1223 748348.
E-mail address: pt290@eng.cam.ac.uk (P.H. Tan).

Stokes and anti-Stokes overtone of the D mode had been discussed in detail for carbon nanotubes, two-dimensional graphite and graphite whiskers [3,8,9]. In this paper, we will discuss the double resonance Raman processes for the Stokes and anti-Stokes components of second-order modes involved two different phonons in graphite materials and explain the above experimental features of second-order modes in graphite whiskers.

2. Double resonance Raman scattering of second-order Raman modes in graphite materials

Except the Raman-active zone-center E_{2g} modes at 42 and 1582(G) cm^{-1}, other first-order Raman modes can be classified as two groups: one is due to an intra-valley double resonance process, such as the D′, L_1 and L_2 modes [2,3,7], the other group results from an inter-valley double resonance process, such as the D modes [1,3,6–9]. How these fundamentals contribute to the experimentally observed second-order dispersive modes? To answer this question, it is necessary to analyze the double resonance Raman process of second-order modes in graphite materials.

Here, we first focus our discussions on a second-order mode whose fundamentals just come from intra-valley double resonance processes. Saito et al. [7] had given the first discussion of the double resonance mechanism in terms of intra-valley process of the first-order dispersive modes in graphite [7]. Instead of one phonon and one defect for a first-order mode, the double resonance process of a second-order mode involves two phonons. We assume

in the later text that the frequency of the second-order mode is ω_{1+2} and this second-order mode has two fundamentals with the frequencies of ω_1 and ω_2 ($\omega_1 > \omega_2$), and δk_1 and δk_2 are two wave vectors associated with two fundamentals, $\delta k_{1,2} = \hbar\omega_{1,2}/A$, and $A = \sqrt{3}\gamma_0 a/2$, where a is graphite lattice constant and $\gamma_0 = 2.90$ eV is the tight-binding overlap integral parameter. Because the photon-excited electron in a double resonance process can be first scattered by emitting (or absorbing) a phonon of ω_1 or ω_2, there are four possible Stokes and anti-Stokes intra-valley double resonance processes for a second-order mode as shown in Fig. 1. If we neglect the trigonal warping effect [12], similar to the case of the double resonance process of a first-order mode [1,6,7]. the wave vector of the fundamental ω_1 in Fig. 1(a) is determined by the electronic wave vectors of two involved resonant electronic states, $|\boldsymbol{q}_1| = |2k_0 - \delta k_1|$, where the vectors $k_0 = \varepsilon_L/(2A)$ and ε_L is the laser energy. Because of the demand of the momentum conservation condition ($\boldsymbol{q}_1 + \boldsymbol{q}_2 = 0$), wave vector $\boldsymbol{q}_2 = -\boldsymbol{q}_1$ and its magnitude $|\boldsymbol{q}_2| = |2k_0 - \delta k_1|$. That says that the wave vector of the fundamental ω_2 that contributes to the second-order mode ω_{1+2} is smaller than that ($|2k_0 - \delta k_2/2|$, or $|2k_0 - \delta k_2|$) of the first-order mode ω_2. For the anti-Stokes process depicted in Fig. 1(a), we can similarly determine the wave vectors of fundamentals ω_1 and ω_2 to be $|2k_0 + \delta k_1|$, and thus, the wave vector of the fundamental ω_2 that contributes to the second-order mode ω_{1+2} at the anti-Stokes side is larger than that ($|2k_0 + \delta k_2/2|$, or $|2k_0 + \delta k_2|$) of the first-order mode ω_2. The same analysis can be applied to other Stokes and anti-Stokes double resonance processes in Figs. 1(b)–(d). Several singularities
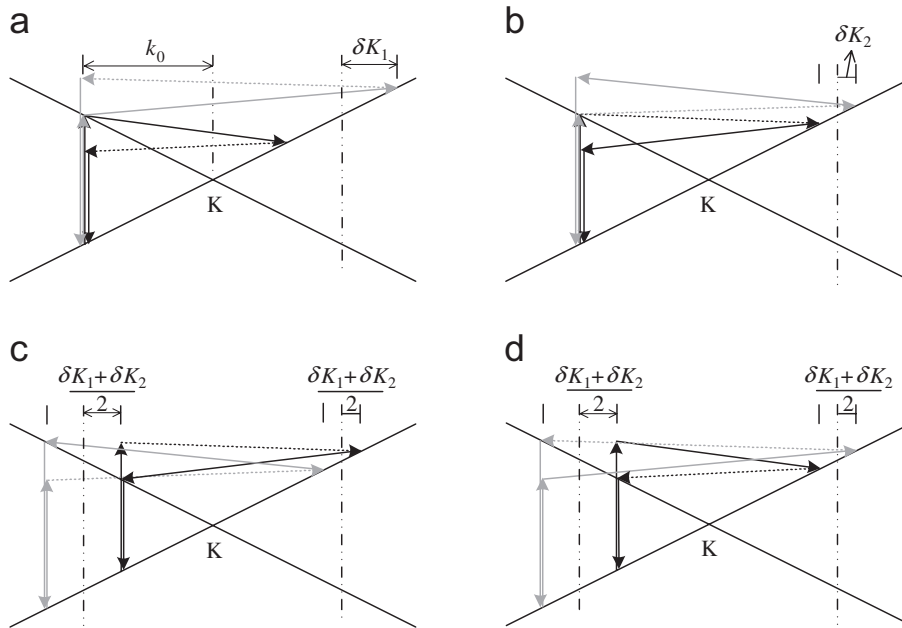
Fig. 1. Schematic diagram of four intra-valley double resonance Stokes (S, black lines) and anti-Stokes (AS, gray lines) processes for a second-order mode in graphite materials: a, inelastic scattering by ω_1 occurs first and the incident states are resonant; b, inelastic scattering by ω_2 occurs first and the incident states are resonant; c, inelastic scattering by ω_2 occurs first and the scattered states are resonant; d, inelastic scattering by ω_1 occurs first and the scattered states are resonant. Here, dashed lines show the scattered or absorbed process of the fundamental with smaller phonon energy.

at $|q_1| = |2k_0 \pm \delta k_2|$, $|q_1| = |2k_0 \pm \delta k_2|$ and $|q_1| = |2k_0 \pm \delta k_1|$ are possible to contribute to the Stokes (−) and anti-Stokes (+) double resonance processes in Figs. 1(b)–(d), respectively.

In short, for the intra-valley double resonance process of a second-order mode ω_{1+2}, its fundamentals ω_1 and ω_2 have equal and opposite phonon wave vectors. The wave vectors of ω_1 and ω_2 have two singularities around

$$|q| = |2k_0 \pm \delta k_2| \quad \text{or} \quad |q| = |2k_0 \pm \delta k_1|, \quad (1)$$

for the Stokes (−) and anti-Stokes (+) Raman scatterings. Therefore, the Stokes and anti-Stokes second-order modes exhibit a two-peak behavior, and the frequency splitting of the two peaks is determined by the frequency values of the fundamentals ω_1 and ω_2 and their dispersive properties. If two singularities at $|2k_0 \pm \delta k_1|$ and $|2k_0 \pm \delta k_2|$ have the same contribution to the Stokes (−) and anti-Stokes (+) Raman scatterings of a second-order mode ω_{1+2} and the frequencies of its fundamentals ω_1 and ω_2 have a linear relation to the excitation energy, the frequencies of the second-order mode at Stokes (−) and anti-Stokes (+) sides, respectively, are

$$\omega_{1+2} = \omega_1 + \omega_2 \pm \hbar(\omega_1 + \omega_2)(\partial\omega_1/\partial e_L + \omega_2/\partial\varepsilon_L)/2, \quad (2)$$

where ω_1 and ω_2 are the frequencies of the first-order modes excited by the laser ε_L. Because the value of $\partial(\omega_1 + \omega_2)/\partial\varepsilon_L$ is much smaller than 1.0, the laser-energy dispersion of the second-order mode is almost equal to the sum of laser-energy dispersions of its fundamentals,

$$\partial\omega_{1+2}/\partial\omega_L \approx \omega_1/\partial\varepsilon_L + \partial\omega_2/\partial\varepsilon_L. \quad (3)$$

The frequency difference between Stokes and anti-Stokes components of the second-order mode can be calculated using Eq. (2) and is expected to be

$$\Delta\omega_{1+2} = \hbar(\omega_1 + \omega_2)\partial(\omega_1 + \omega_2)/\partial\varepsilon_L \approx \hbar\omega_{1+2}\partial\omega_{1+2}/\partial\varepsilon_L. \quad (4)$$

The above analysis can also be applied to the inter-valley double resonance Raman process of a second-order mode, which is responsible to observe the 2D overtone [3,7–9]. The wave vector selection rule Eq. (1) of the intra-valley double resonance Raman process of a second-order mode can also be used to the inter-valley double resonance process after replacing the vector q in Eq. (1) with $q-K$.

Overtone is one special case of the second-order mode that its fundamentals have the same frequency ($\omega_1 = \omega_2$). In this case, the four Raman processes in Fig. 1 are simplified into two possible processes in the double resonance Raman process [3,7–9]. The wave vectors of its fundamentals ω_1 have only one singularity around $2k_0 \pm \delta k_1$ from Γ (intra-valley DRRS) or K (inter-valley DRRS) point for the Stokes (−) and anti-Stokes (+) Raman scatterings. Then, the frequencies of the overtone at Stokes (−) and anti-Stokes (−) sides, respectively, are

$$\omega_{1+1} = 2\omega_1 \pm 2\hbar\omega_1\omega_1/\partial\varepsilon_L. \quad (5)$$

The laser-energy dispersion and the frequency difference between Stokes and anti-Stokes components of the over-

tone, respectively, are expected to be

$$\partial\omega_{1+1}/\partial\varepsilon_L \approx 2\partial\omega_1/\partial\varepsilon_L, \quad \Delta\omega_{1+1} = 4\hbar\omega_1\omega_1/\partial\varepsilon_L. \quad (6)$$

3. Discussions on the second-order Raman modes in graphite whiskers

Based on the above analysis, the frequencies of Stokes and anti-Stokes components of a second-order Raman mode can be quantitatively calculated from the frequencies of its first-order fundamentals and their laser-energy dispersive properties. Here, we apply this to second-order modes in an individual graphite whisker, which had been published elsewhere [2].

Raman results in graphite whiskers [2,3] show that the phonons around the wavevector of $q = 2k_0 - \delta k$ will contribute to the D′ and L_1 modes at the Stokes side. We use ω_1 (ω_2) and δk_1 (δk_2) to stand for the frequency and vector of the first-order L_1 (D′) mode, and thus $\omega_1 = \omega_1(2k_0 - \delta k_1) = 228 \, \text{cm}^{-1}$ and $\omega_2 = \omega_2(2k_0 - \delta k_2) = 1618 \, \text{cm}^{-1}$ for a 632.8 nm excitation. Then, we can get $\omega_1(2k_0 - \delta k_2) = \omega_1 - \hbar(\omega_2 - \omega_1)\partial\omega_1/\partial\varepsilon_L = 205.7 \, \text{cm}^{-1}$ and similarly $\omega_2(2k_0 - \delta k_1) = 1619.6 \, \text{cm}^{-1}$. These values are summarized in Table 1 along with the experimental results. The average value of the $L_1 + $ D′ mode associated with phonon wave vectors of $2k_0 - \delta k_{1,2}$ for Stokes scattering is in excellent agreement with the observed frequencies at $1833 \, \text{cm}^{-1}$, respectively [2]. This suggests that the mode observed at $1833 \, \text{cm}^{-1}$ is a combination of the L_1 and D′ modes.

Using the double resonance Raman mechanism for second-order Raman modes, we calculate the Stokes frequencies of second-order Raman modes observed in graphite whiskers excited by 632.8 nm excitation and summary the results in Table 2. According to the calculated results, the modes observed at 1833 and $1951 \, \text{cm}^{-1}$, respectively, are designated as $L_1 + $ D′ and $L_2 + $ D′ modes.

Table 1
Average theoretical Stokes frequencies $\bar{\omega}_{1+2}$ (th) and experimental Stokes frequencies ω_{1+2}(exp) (in cm^{-1}) of the $L_1 + $ D′ mode

Vector	ω_1 (L_1)	ω_2 (D′)	ω_1 (L_1) + ω_2 (D′)	$\bar{\omega}_{1+2}$ (th)	ω_{1+2} (exp)
$2k_0 - \delta k_1$	228.0	1619.6	1847.6	1835.6	1833
$2k_0 - \delta k_2$	205.7	1618.0	1823.7		

The frequencies of its fundamentals $L_1(\omega_1)$ and D′(ω_2) modes associated with two possible double resonance Raman processes and their sum $(\omega_1 + \omega_2)$ are also shown.

Table 2
Theoretical (th) and experimental (exp) Stokes frequencies (in cm^{-1}) of second-order Raman modes in graphite whiskers

Assignment	$2L_1$	$L_1 + L_2$	$L_1 + $ D′	$L_2 + $ D′	2D	2D′
ω (th)	456	578	1836	1951	2666	3236
ω (exp)	452	570	1833	1951	2662	3237

Table 3
Theoretical (th) and experimental (exp) values of the dispersions $\partial\omega/\partial\varepsilon_L$ (in cm^{-1}/eV) and frequency difference between Stokes and anti-Stokes components $\Delta\omega = |\omega_{AS}| - |\omega_S|$ (in cm^{-1}) of a second-order Raman mode in graphite whiskers

Assignment	$2L_1$	$L_1 + L_2$	$L_1 + D'$	$L_2 + D'$	$2D$	$2D'$
$\partial\omega/\partial\varepsilon_L$ (th)	258	345	139	226	92	18
$\partial\omega/\partial\varepsilon_L$ (exp)			140	224	95	18
$\Delta\omega$ (th)	14.5	24.4	31.6	55.2	30.4	7.2
$\Delta\omega$ (exp)	15	23	33	53	34	8

The theoretical calculated frequencies for all the second-order modes in Table 2 are in well agreement with the experimental ones, which further confirm the assignment for the observed second-order modes. One point to be pointed out here is that we do not do the symmetry analysis for the second-order modes [1], because we observed the symmetry-forbidden combination $L_1 + L_2$ mode [2] whose two fundamentals belong to phonon branches with different symmetries, but its intensity is comparable to that of the $2L_1$ mode.

The laser-energy dispersions and frequency difference between Stokes and anti-Stokes sides of second-order Raman modes in graphite whiskers are also calculated based on the Raman results of first-order Raman modes and are summarized in Table 3. The theoretical results are also consistent with the experimental results very well, such as the frequency difference for an overtone in the Stokes and anti-Stokes sides is about four times as large as the frequency difference of its fundamental [2,11]. The calculated result of Eq. (4), which shows that the frequency difference of Stokes and anti-Stokes second-order mode is determined by the frequency and dispersive properties of the second-order mode, which also confirms to the experimental results of second-order modes in graphite whiskers. Because the laser-energy dispersions and Stokes/anti-Stokes frequency difference of second-order Raman modes are directly related to the corresponding properties of its fundaments as Eqs. (3) and (4), double resonant Raman mechanism of second-order Raman modes provide a new method to assign the observed second-order Raman modes in graphite materials.

4. Results

We have discussed the double resonance Raman scattering mechanism of Stokes and anti-Stokes second-order modes in graphite materials. If the two fundamentals of a second-order mode are dispersive, the phonon wave vector of one fundamental mode is determined by the double incident or scattered resonance process, and that of another fundamental mode is chosen by the momentum conservation condition. A combination mode in graphite materials is composed of two peaks whose frequency splitting is determined by the frequency difference and dispersive properties of its two fundamentals. For an overtone, its Stokes and anti-Stokes components only exhibit a single peak. Double resonance Raman scattering can be applied to quantitatively explained all the observed results of second-order Raman modes in graphite whiskers.

Acknowledgments

References

[1] S. Reich, C. Thomsen, Philos. Trans. Roy. Soc. A 362 (2004) 2271.
[2] P.H. Tan, C.Y. Hu, J. Dong, W. Shen, B. Zhang, Phys. Rev. B 64 (2001) 214301.
[3] P.H. Tan, L. An, L.Q. Liu, Z.X. Guo, R. Czerw, D.L. Carroll, P.M. Ajayan, N. Zhang, H.L. Guo, Phys. Rev. B 66 (2002) 245410.
[4] R.P. Vidano, D.B. Fishbach, L.J. Willis, T.M. Loehr, Solid. State Commun. 39 (1981) 341.
[5] Y. Kawashima, G. Katagiri, Phys. Rev. B 52 (1995) 10053.
[6] C. Thomsen, S. Reich, Phys. Rev. Lett. 85 (2000) 5214.
[7] R. Saito, A. Jorio, A.G. Souza Filho, G. Dresselhaus, M.S. Dresselhaus, M.A. Pimenta, Phys. Rev. Lett. 88 (2002) 027401.
[8] V. Zólyomi, J. Kürti, Phys. Rev. B 66 (2002) 073418;
V. Zólyomi, J. Kürti, A. Grüneis, H. Kuzmany, Phys. Rev. Lett. 90 (2003) 157401.
[9] L.G. Cancado, M.A. Pimenta, R. Saito, A. Jorio, L.O. Ladeira, A. Grueneis, A.G. Souza-Filho, G. Dresselhaus, M.S. Dresselhaus, Phys. Rev. B 66 (2002) 035415.
[10] P.C. Eklund, J.M. Holden, R.A. Jishi, Carbon 33 (1995) 959.
[11] P.H. Tan, Y.M. Deng, Q. Zhao, Phys. Rev. B 58 (1998) 5435.
[12] R. Saito, G. Dresselhaus, M.S. Dresselhaus, Phys. Rev. B 61 (2000) 2981.